Structural Eng./Earthquake Eng. Vol. 8, No. 2, 55s-62s, July 1991
Japan Society of Civil Engineers (Proc. of JSCE No. 432/ I -16)

EARTH PRESSURE ANALYSIS OF FILLED MATERIALS BY DISTINCT ELEMENT METHOD USING ELLIPSE MODEL

Satoshi KATSUKI*
and Nobutaka ISHIKAWA**

This paper presents an earth pressure analysis of filled materials of the steel-made Sabo structure by using the distinct element method. The filled materials are firstly assumed as ellipse models in the distinct element method. Then, the contact force between two ellipse elements is calculated by using the Newton's method and the difference equation of motion for the ellipse models is numerically solved by employing the Euler's method. Finally, the earth pressure of filled boulder is found by summing up the contact force applying to the steel wall. The three examples are analyzed to illustrate the validity and application of this approach.

Keywords : *distinct element method, earth pressure analysis, ellipse model, filled materials*

1. INTRODUCTION

Recently the steel-made Sabo structures have been built in many places where erosion and volcanic debris flow are seemed to be occurred. For instance, a number of steel-made Sabo structures have been adopted at Usu volcanic mountain area, Hokkaido and Sakurajima volcanic mountain area, Kagoshima in Japan. The steel framed Sabo structures with fill materials have been designed by using the following two methods in the current design procedure[1].

One method is to design the structure by taking into account for only shearing resistance of filled materials without frame, and the other method is to design it by considering only the resistance of steel frame without fill materials. In each method it is necessary to evaluate how much the value of the coefficient of earth pressure at rest should be taken for the various kinds and arrangements of fill materials.

There are, however, quite few studies on the earth pressure of the fill materials, except the pressure analysis[2] of rock-like granular materials in silo by the distinct element method (DEM) using circle particles[3)~6].

To this end, this study presents the earth pressure analysis of filled materials in the steel framed Sabo structure by using the DEM. The method firstly assumes the particles as the ellipse model by considering the shape anisotropy of boulder or gravel etc.. Then, the contact force between two ellipse elements is calculated by adopting Newton's method and the difference equation of motion for the ellipse model is solved by making use of Euler's method. Therefore, the earth pressure of fill materials against frame wall can be found by summing up the contact force. The influences of arrangement and shape anisotropy on the earth pressure of filled material against the frame wall are examined. Finally, the effect of arrangement of particles under the back storage sand pressure on the earth pressure of filled materials and the movement of elements is studied.

The following assumptions are made in this study.

(1) A particle of the filled materials is assumed as an ellipse model which is a rigid body.

(2) The normal and tangential springs and dashpots exist between two particles.

(3) The tangential spring is assumed as the elastic-perfectly plastic model for the slip condition.

2. DISTINCT ELEMENT METHOD USING ELLIPSE MODEL

The distinct element method (DEM) proposed by Cundall[3] can analyze the behavior of the soil mass from the state of motion to the state of rest by solving the equation of motion numerically. In this section the distance and the contact force between two ellipse elements are firstly derived and then, the earth pressure analysis procedure is developed.

(1) Distance between two ellipse elements

Consider two ellipse elements i and j with the local coordinates (X_1, Y_1) and (X_2, Y_2) as shown in **Fig.1**. Using these local coordinates (X_1, Y_1) and (X_2, Y_2), the points on the boundary lines of the

* Member of ISCE, Dr.Eng., Research Associate, Dept. of Civil Engineering, National Defense Academy (1-10-20 Hashirimizu, Yokosuka, 239, Japan)
** Member of JSCE, Dr.Eng., Professor, Dept. of Civil Engineering, National Defense Academy

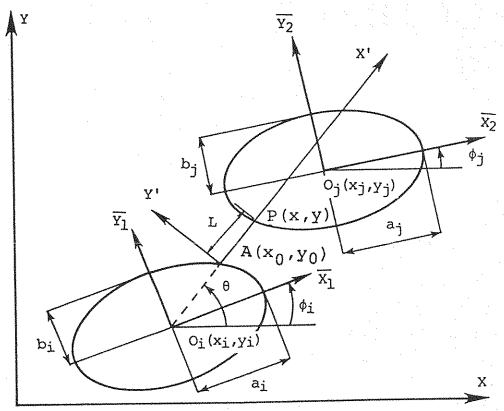

Fig.1 Distance between two ellipse elements.

two ellipse elements i and j are expressed, respectively, as follows :

$$\frac{\overline{x_1}^2}{a_i^2}+\frac{\overline{y_1}^2}{b_i^2}=1 \quad \cdots\cdots(1\text{-a})$$

$$\frac{\overline{x_2}^2}{a_j^2}+\frac{\overline{y_2}^2}{b_j^2}=1 \quad \cdots\cdots(1\text{-b})$$

where,

a_i, a_j : the lines of apsides of the ellipse elements i and j,

b_i, b_j : the minor axes of the ellipse elements i and j,

$\overline{x_1}, \overline{y_1}$: the local coordinate values on the boundary line of the ellipse element i,

$\overline{x_2}, \overline{y_2}$: the local coordinate values on the boundary line of the ellipse element j,

Herein, consider the contact problem between two ellipse elements as shown in **Fig.1**. The contact is defined as the existing of the intersecting points between two elements i and j. However, it is very difficult to get the intersecting points by solving Eqs.(1-a) and (1-b) of two ellipse elements, directly. Therefore, the distance L between two ellipse elements i and j is defined by the following procedure.

Consider an arbitrary point $A(x_0, y_0)$ on the boundary line of the ellipse element i. Then, make the arbitrary local coordinate (X', Y') in which the X'-axis is the extended line connecting the center point $O_i(x_i, y_i)$ with the arbitrary point $A(x_0, y_0)$ and the Y' -axis is the line with the origin $A(x_0, y_0)$ at the right angle to the X' -axis.

Now, express the point on the boundary line of the ellipse elements j by the local coordinate (X', Y').

At first, the local coordinate value $(\overline{x_1}, \overline{y_1})$ of the boundary line on the ellipse element i is also expressed by using Eq. (A-6) in Appendix I as follows :

$$\left.\begin{aligned}\overline{x_1}&=a_i\cos[\tan^{-1}\{(a_i/b_i)\tan(\theta-\phi_i)\}]\\ \overline{y_1}&=b_i\sin[\tan^{-1}\{(a_i/b_i)\tan(\theta-\phi_i)\}]\end{aligned}\right\} \cdots\cdots(2)$$

where,

θ : an arbitrary angle between the X' -axis and X-axis which is the global coordinate,

ϕ_i : the angle between the X_1-axis which is the line of apsides of element i and the X-axis.

Then, by transforming the coordinate from the local coordinate value $(\overline{x_1}, \overline{y_1})$ to the global coordinate (X, Y), an arbitrary point $A(x_0, y_0)$ on the boundary line of the element i is expressed as follows :

$$\left.\begin{aligned}x_0&=\overline{x_1}\cos\phi_i-\overline{y_1}\sin\phi_i+x_i\\ y_0&=\overline{x_1}\sin\phi_i+\overline{y_1}\cos\phi_i+y_i\end{aligned}\right\} \cdots\cdots(3)$$

On the other hand, an arbitrary point $P(x, y)$ on the boundary line of the ellipse element j is expressed by using the local coordinate value (x', y') as follows :

$$\left.\begin{aligned}x&=x'\cos\theta-y'\sin\theta+x_0\\ y&=x'\sin\theta+y'\cos\theta+y_0\end{aligned}\right\} \cdots\cdots(4)$$

where,

x, y : the value of the boundary line on the ellipse element j in the global coordinate (X, Y),

x', y' : the value of the boundary line on the ellipse element j in the local coordinate (X', Y')

This point $P(x, y)$ can be also written by using the local coordinate value $(\overline{x_2}, \overline{y_2})$ in which the origin exist in the center point of the ellipse element j as follows :

$$\left.\begin{aligned}x&=\overline{x_2}\cos\phi_j-\overline{y_2}\sin\phi_j+x_j\\ y&=\overline{x_2}\sin\phi_j+\overline{y_2}\cos\phi_j+y_j\end{aligned}\right\} \cdots\cdots(5)$$

where,

$\overline{x_2}, \overline{y_2}$: the arbitrary point value of the boundary line on the ellipse element j in the local coordinate (X_2, Y_2),

ϕ_j : the angle between the X_2-axis which is the line of apsides of element j and X-axis.

Therefore, eliminating the global coordinate value (x, y) from Eqs. (4) and (5), the local coordinate value $(\overline{x_2}, \overline{y_2})$ of the element j can be expressed as the function of the arbitrary local coordinate value (x', y') as follows :

$$\left.\begin{aligned}\overline{x_2}&=x'\cos\beta-y'\sin\beta+R\cos\gamma\\ \overline{y_2}&=x'\sin\beta+y'\cos\beta+R\sin\gamma\end{aligned}\right\} \cdots\cdots(6)$$

where,

$$\left.\begin{aligned}R&=\sqrt{(x_0-x_j)^2+(y_0-y_j)^2}\\ x_0&=a_i\cos\alpha\cos\phi_i-b_i\sin\alpha\sin\phi_i+x_i\end{aligned}\right|$$

$$\left.\begin{aligned} y_0 &= a_i \cos\alpha \cos\phi_i + b_i \sin\alpha \sin\phi_i + y_i \\ \alpha &= \tan^{-1}[(a_i/b_i)\tan(\theta-\phi_i)] \\ \beta &= \theta-\phi_j \\ \gamma &= \tan^{-1}[(y_0-y_j)/(x_0-x_j)]-\phi_j \end{aligned}\right\} \cdots (7)$$

Furthermore, substituting Eq.(6) into Eq.(1-b), the points on the boundary line of the ellipse element j are expressed by using the arbitrary local coordinate (X', Y') as follows :

$$\frac{(X'\cos\beta - Y'\sin\beta + R\cos\gamma)^2}{a_j^2} + \frac{(X'\sin\beta + Y'\cos\beta + R\sin\gamma)^2}{b_j^2} = 1 \quad \cdots (8)$$

Therefore, the distance L between the element i and j can be derived by substituting $Y'=0$ in Eq.(8) and solving the quadratic equation with respect to X' as follows :

$$X' = L = \frac{-(a_j^2 R\sin\beta\sin\gamma + b_j^2 R\cos\beta\cos\gamma)}{(a_j^2\sin^2\beta + b_j^2\cos^2\beta)} - \frac{\sqrt{(a_j^2 R\sin\beta\sin\gamma + b_j^2 R\cos\beta\cos\gamma)^2 - (a_j^2\sin^2\beta + b_j^2\cos^2\beta)(a_j^2 R^2\sin^2\gamma + b_j^2 R^2\cos^2\gamma - a_j^2 b_j^2)}}{(a_j^2\sin^2\beta + b_j^2\cos^2\beta)} \quad \cdots (9)$$

(2) Contact judgement

The distance L of Eq.(9) is not the true distance between the two elements i and j, because the angle θ in Eq.(9) is not unknown yet. Therefore, the minimum value of the distance L is required to be taken with respect to the angle θ.

Herein, the contact between two elements i and j is judged by the condition that the true distance (min L) becomes zero or negative. That is,

$$\min L(\theta) \leqq 0 \quad \cdots (10)$$

where,

$\min L(\theta)$: the minimum value of the distance L with respect to the angle θ

The angle θ when the distance L becomes the minimum value is obtained by following condition.

$$dL(\theta)/d\theta = 0 \quad \cdots (11)$$

Eq.(11) can be solved numerically by using the Newton's method.

(3) Contact point and contact angle

Consider the element i approaching to the element j from the time $t-\Delta t$ to the time t as shown in **Fig.2**.

It is assumed that the contact point between two elements is given at the intermediate point of the intersecting line $\overline{P_1P_2}$, when the boundary lines of elements i and j intersect each other at points P_1 and P_2 at the time t as shown in **Fig.2**. Herein, the

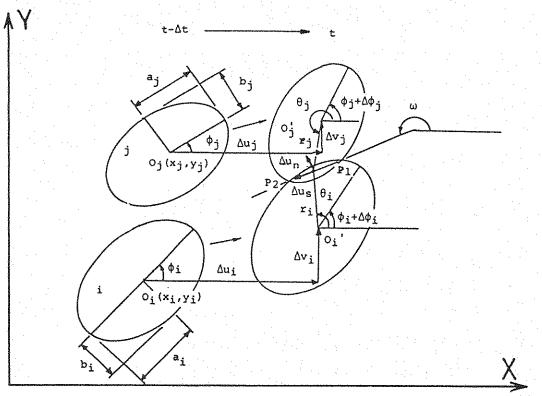

Fig.2 Contact judgement between two ellipse elements.

contact angle is defined as the angle ω between the global X-axis and the intersecting line $\overline{P_1P_2}$. It is noted that the point values P_1 and P_2 can be found by solving the equation $L(\theta)=0$ using the Newton's method.

It is also assumed that the angle θ_1 of P_1 is always smaller than the one of P_2. Futhermore, it is also noted that the contact angle ω is taken as shown in **Fig.2**, but the contact angle is given as $\omega' = \omega - \pi$ if the elements i and j are upside down.

(4) Displacement increments at contact point

When the two ellipse elements i and j are approaching each other from time $t-\Delta t$ to time t as shown in **Fig.2**, the normal and tangential displacement increments Δu_n (positive if two elements approach) and Δu_s (positive if the element rotates unclockwise) can be expressed as follows :

$$\Delta u_n = (\Delta u_i - \Delta u_j)\sin\omega - (\Delta v_i - \Delta v_j)\cos\omega - r_i\Delta\phi_i\cos(\theta_i-\omega) + r_j\Delta\phi_j\cos(\theta_j-\omega) \quad \cdots (12)$$

$$\Delta u_s = (\Delta u_i - \Delta u_j)\cos\omega + (\Delta v_i - \Delta v_j)\sin\omega - r_i\Delta\phi_i\sin(\theta_i-\omega) + r_j\Delta\phi_j\sin(\theta_j-\omega) \quad \cdots (13)$$

where, Δu_i, Δu_j are the horizontal displacement increments at the center of elements i and j, respectively ; Δv_i, Δv_j are the vertical displacement increments at the center of elements i and j, respectively ; $\Delta\phi_i$, $\Delta\phi_j$ are the rotation increments at the center of elements i and j, respectively ; r_i, r_j are the lengths from the center of the elements i and j to the contact point, respectively.

(5) Contact force

It should be noted that the elastic springs and the dashpots are assumed at the contact point in the normal and tangential directions as shown in **Fig.3**. Therefore, the contact forces can be divided into

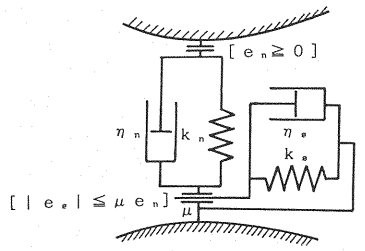

Fig.3 Spring and dash-pot at contact point.

the components of the normal force and the tangential force (positive if the element rotates clockwise).

a) Normal contact force

The normal contact force at the time t can be found by the spring force and the viscous damping force as follows:

$$[f_n]_t=[e_n]_t+[d_n]_t \quad \cdots\cdots (14)$$

in which,

$$[e_n]_t=[e_n]_{t-\Delta t}+\Delta e_n$$

$$[d_n]_t=\Delta d_n$$

$$\Delta e_n=k_n\Delta u_n$$

$$\Delta d_n=\eta_n\Delta u_n/\Delta t$$

f_n : the total force at contact point in the normal direction, e_n : the spring force in the normal direction, d_n : the damping force in the normal direction, Δ : increment from $t-\Delta t$ to t, k_n : the spring coefficient in the normal direction, η_n : the damping coefficient in the normal direction.

It is noted that the spring has no tension force between two elements. That is,

$$[e_n]_t=[d_n]_t=0 \quad \text{if} \quad [e_n]_t<0 \quad \cdots\cdots (15)$$

b) Tangential contact force

The tangential contact force can be calculated by the following equation.

$$[f_s]_t=[e_s]_t+[d_s]_t \quad \cdots\cdots (16)$$

where,

$$[e_s]_t=[e_s]_{t-\Delta t}+\Delta e_s$$

$$[d_s]_t=\Delta d_s$$

$$\Delta e_s=k_s\Delta u_s$$

$$\Delta d_s=\eta_s\Delta u_s/\Delta t$$

f_s : the total force at the contact point in the tangential direction, e_s : the spring force in the tangential direction, d_s : the damping force in the tangential direction, k_s : the spring coefficient in the tangential direction, η_s : the damping coefficient in the tangential direction.

It is also noted that the tension force is not considered and the sliding effect is taken into account as follows:

$$[e_s]_t=[d_s]_t=0 \quad \text{if} \quad [e_n]_t<0 \quad \cdots\cdots (17)$$

$$\left.\begin{aligned}&[e_s]_t=\mu[e_n]_t\times \mathrm{SIGN}([e_s]_t),\\ &\text{and } [d_s]_t=0 \quad \text{if} \quad [e_s]_t>\mu[e_n]_t\end{aligned}\right\} \quad \cdots\cdots (18)$$

where, μ is the coefficient of friction and SIGN(Z) is the sign of variable Z.

As for the constant values k and η, the following equations are derived by using the radius r_1 and r_2 at the contact point[2].

$$\left.\begin{aligned}k_n&=\frac{\pi E}{2(1-\nu^2)\{2/3+\ln(4r_1/B)+\ln(4r_2/B)\}}\\ k_s&=k_n\cdot s\\ \eta_n&=2\sqrt{mk_n}\\ \eta_s&=\eta_n\cdot\sqrt{s}\end{aligned}\right\} \quad \cdots\cdots (19)$$

where,

s : the ratio of the tangential spring coefficient to normal one ; m : the mass of element ; B : the contact width.

It is assumed that the contact width B is given by the length between two contact points P_1 and P_2 in **Fig.2** and the radius r_1 and r_2 are given as the radius of curvature at the contact point which is obtained by the following equations.

$$r_i=\frac{|(a_i^2\sin^2\lambda_i+b_i^2\cos^2\lambda_i)^{3/2}|}{a_ib_i} \qquad (i=1, 2)$$

$$\lambda_i=\tan^{-1}\left\{\frac{a_i}{b_i}\tan(\theta_i-\phi_i)\right\} \qquad (i=1, 2)$$

(6) Equation of motion

For particle i, forces are summed over all particles contacting with the particle i. Therefore, the equations of motion for particle i are expressed as follows:

$$\frac{\partial^2u_i}{\partial t^2}=\frac{1}{m_i}[X_i]_t \quad \cdots\cdots (20)$$

$$\frac{\partial^2v_i}{\partial t^2}=\frac{1}{m_i}[Y_i]_t \quad \cdots\cdots (21)$$

$$\frac{\partial^2\phi_i}{\partial t^2}=\frac{1}{I_i}[M_i]_t \quad \cdots\cdots (22)$$

where,

$$[X_i]_t=\sum_j\{-[f_n]_t\sin\omega-[f_s]_t\cos\omega\}$$

$$[Y_i]_t=\sum_j\{[f_n]_t\cos\omega-[f_s]_t\sin\omega-m_ig\}$$

$$[M_i]_t=\sum_j\{([f_n]_t\sin\omega+[f_s]_t\cos\omega)r_i\sin\theta_i+([f_n]_t\cos\omega-[f_s]_t\sin\omega)\cdot r_i\cos\theta_i\}$$

in which $\sum_j$ means the sum over all particles j contacting with the particle i and m_ig is the gravity of particle i. In order to solve Eqs.(20)~(22), the Euler's method[7] can be adopted by making the difference of them at time increment Δt, numerically.

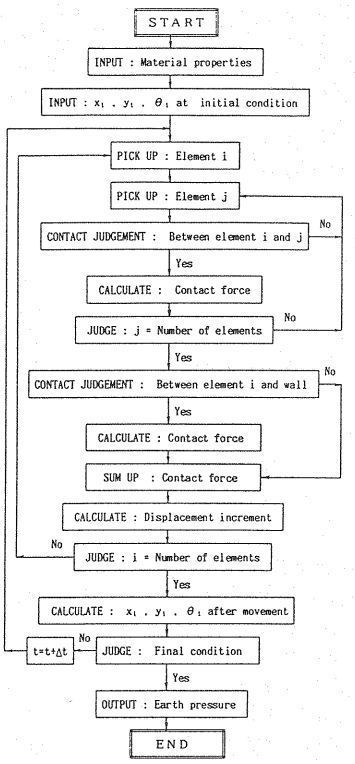

Fig.4 Analysis procedure.

Herein, the following two items are the features of the ellipse element which are different from the circle element. At first, it is noted that the normal and tangential displacement increments $\Delta u_n, \Delta u_s$ are affected by the rotation increments $\Delta\phi_i, \Delta\phi_j$ in Eqs.(12), (13) and, as such, the rotational movement causes the normal and tangential displacements.

Then, it is also noted that the rotational force M_i is influenced by the normal and tangential contact forces f_n, f_s in Eq.(22) and, therefore, the normal contact force as well as the tangential force causes the rotational force. In the case of circle element, the rotational movement does not cause the normal displacement, and the normal force can not cause the rotational force.

(7) Analysis procedure

Fig.4 shows the analysis procedure by the distinct element method. In this method the contact judgement is limited on the neighboring elements by considering the rule of arrangement.

3. NUMERICAL EXAMPLES

(1) Example 1 :

In order to illustrate the validity of the approach, the earth pressure of 179 circle elements ($a_i = b_i = a_j = b_j = r$) in the frame with the length $L = 2.0$ m is calculated in the condition subjected to the self-weight of all particles. The radius of circle element is $r = 7.0$ cm and the material constants are density $\rho = 2.69$ gf/cm^3, Poisson's ratio $\nu = 0.3$, Young's modulus $E = 750$ kgf/cm^2, the ratio $s = 0.25$ and frictional coefficient $\mu = 0.577$ (the friction angle $= 30°$). Where, those values are reffered to the parameters of the reference 2).

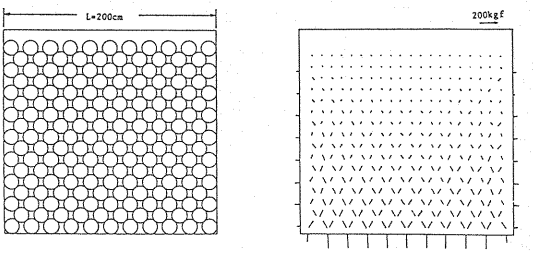

(a) Element arrangement after filling

(b) Contact force after filling

Fig.5 179 circle elements.

The calculation has been begun from the uncontact condition between elements and completed to the rest condition by using the time increment $\Delta t = 10^{-4}$ sec. **Fig.5** (b) shows the earth pressure at the contact point of each element as the resultant vector of contact force.

It is confirmed from **Fig.5** (b) that the sum of the horizontal forces is equal to zero and the sum of vertical forces is equal to the self-weight of all particles, respectively. It is also noted that the qualitative result of **Fig.5** (b) is agreed with the ones obtained by Kiyama *et al.*[2] and, as such, this algorithm is valid for the earth pressure analysis of fill materials in the frame.

(2) Example 2 :

In order to examine the effect of the shape anisotropy, the four different types of particles as shown in **Fig.6** (a) have been calculated by using the same material constants as Example 1.

Fig.6 (b) shows the relation between the height of side wall and the earth pressure of filled materials. It is found from **Fig.6** (b) that the earth pressure in the arrangement of the flat shape of particles (pattern A or B) is smaller than the one in the case of the longitudinal shape of particles (pattern D).

It is also noted that the earth pressure at the bottom becomes smaller than the upper part, since the bottom force is influenced by the friction of the bottom plate.

In these cases, the earth pressure is affected by both of the shape anisotropy and element arrangement. Here, the contact angle ω is defined as the parameter considering simultaneously

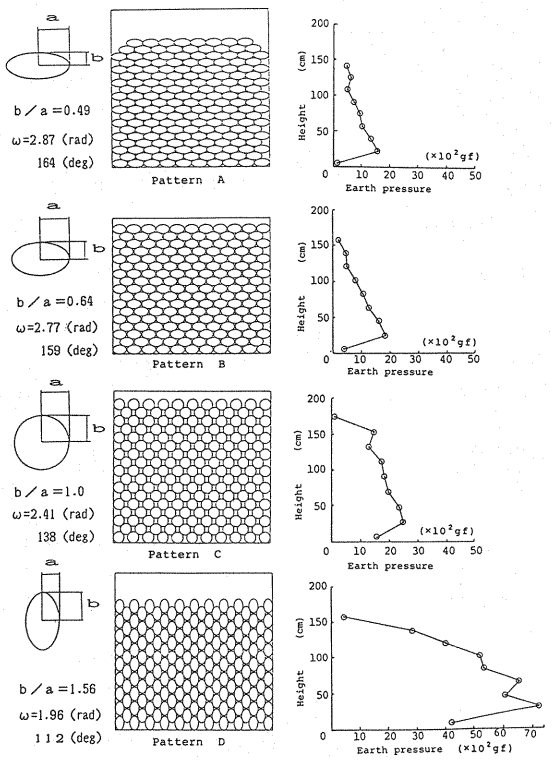

(a) Element arrangement after filling

(b) Relation between height and earth pressure

Fig.6 Earth pressure of side wall at natural pile of filled materials.

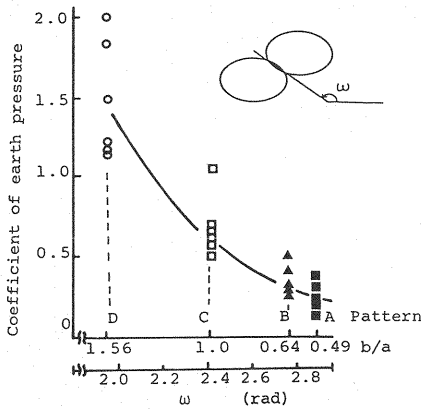

Fig.7 Relation between earth pressure coefficient and contact force angle ω.

both of the shape anithotropy and the element arrangement. Therefore, the relationship between the earth pressure and the contact angle ω has been examined.

Fig.7 shows the relation between the coefficient of earth pressure and the contact angle ω. The coefficient of earth pressure is calculated as follows :

$$K=\frac{\sigma_H}{\sigma_v}=\frac{P_h/d}{\sigma_{v\max}\cdot h/H} \quad \cdots\cdots (23)$$

in which, P_h is the contact force of the element contacting to the wall ; d is the mean distance between the elements contacting to the wall ; $\sigma_{v\max}$ is the vertical pressure at the bottom due to the whole filled materials ; h is the height from the bottom plate to the element corresponding to the contact force P_h ; H is the height of whole filled materials.

It is found from **Fig.7** that the coefficient of earth pressure becomes $K=0.2\sim0.3$ in the case of pattern A, $K=0.6$ in pattern C and $K=1.2\sim2.0$ in pattern D.

It is also noted that the coefficient of the earth pressure is dispersed because of the use of DEM, although it should be constant in the case of the Rankine's theory.

(3) Example 3 :

The steel-made Sabo dam is generally subjected to the horizontal force from back wall as a back storage sand pressure. Herein, in order to examine the case subjected to the back storage sand pressure, the earth pressure to the wall has been calculated by changing the arrangement and angle of particles as shown in **Fig.8** (a). It is assumed that the back storage sand pressure directly applies to the back side boulders as shown **Fig.8** (b), and the steel frame is modeled as the rigid rectangular frame. **Fig.8** (b) shows the earth pressure at the contact point of particle as similar manner as Example 1.

It is found from **Fig.8** (b) that the earth pressures in the case of patterns A and B have diagonal force to the lower direction and become larger at the bottom in the frame. In the case of pattern C the contact force becomes larger at the upper part in the front wall. It should be noted, however, that the contact force of pattern D is diagonal force to the lower direction in a similar way as patterns A and B. On the other hand, it is found from pattern E in **Fig.8** (b) that the earth pressure to the front wall is uniform at each height in the frame.

Consequently, the earth pressure transmission in the patterns A, B and D change direction of principal pressure from horizontal to the lower direction, but the one in the patterns C and E can not change the direction of principal pressure. Therefore, the pressures in the front wall of patterns A, B and D are smaller than those in the case of patterns C and E, respectively. Furthermore, **Fig.8** (c) shows the relation between the wall height and the front wall earth pressure per back storage sand pressure. It is also found from

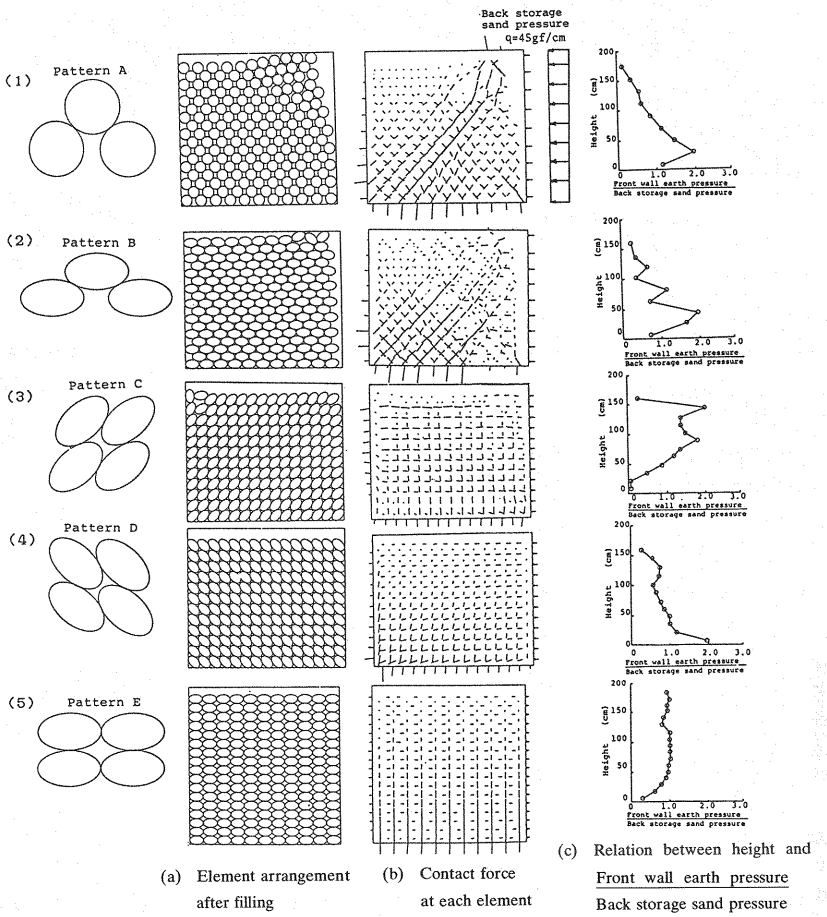

Fig.8 Earth pressure of elements under back storage sand pressure.

Fig.8 (c) the earth pressure in the patterns A, B, D shows a triangular distribution. This means that patterns A, B, D are good arrangements for the frame because the frame resists as a cantilever in the case of back sand pressure and the resistance in the upper part of the front wall is smaller than the one in the lower part.

4. CONCLUSIONS

The following conclusions are drawn from this study.

(1) By introducing the ellipse model in the DEM, the earth pressure can be analyzed for the fill material in the steel frame Sabo structures.

(2) The computational validity of this method has been confirmed by using 179 circle elements.

(3) The earth pressure in the arrangement with particles of flat shape is even smaller than the one in the case with particles of longitudinal shape.

(4) It should be noted that the coefficient of earth pressure becomes $K = 0.2 \sim 0.3$ in the flat shape arrangement, and $K = 0.6$ in the circle shape arrangement.

(5) In the case of the uniform sand pressure, the earth pressure in the flat arrangement of particles becomes diagonal force to the lower direction and, therefore, it is very efficient arrangement because of the smaller resistance in the upper part of the front wall.

ACKNOWLEDGEMENTS: The authors are indebted to Mr. D. Kajimoto for his help in the numerical calculation and to the computer center of the National Defense Academy for the use of computer HITAC M-200H.

APPENDIX I

The point on the boundary line of ellipse model is usually expressed by using the polar coordinate as shown in **Fig.A-1** as follows :

$$x = a \cos \theta' \quad \cdots\cdots\cdots\cdots\cdots\cdots\cdots\cdots \text{(A-1a)}$$

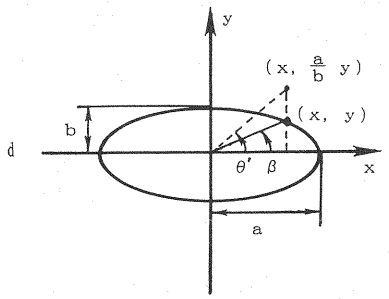

Fig.A-1 Ellipse in the polar coordinate.

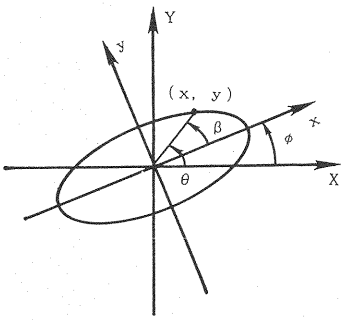

Fig.A-2 Ellipse in the rotate coordinate.

$$y=b\sin\theta' \cdots\cdots (A\text{-}1b)$$

where, θ': the dummy angle variable which is defined by the following equation (A-3).

Dividing Eq.(A-1b) by Eq.(A-1a), the ratio of y to x is given.

$$\frac{y}{x}=\frac{b}{a}\tan\theta' \cdots\cdots (A\text{-}2)$$

Therefore,

$$\theta'=\tan^{-1}\left(\frac{y}{x}\frac{a}{b}\right) \cdots\cdots (A\text{-}3)$$

On the other hand, y/x also can be expressed by using the angle β as shown in **Fig.A**-1 as follows :

$$\frac{y}{x}=\tan\beta \cdots\cdots (A\text{-}4)$$

where, β: the angle between the line which connect the origin point with the arbitrary point (x, y) and x-axis, i.e. the apsides of the ellipse element.

Substituting Eq.(A-4) into Eqs. (A-1), (A-2), (A-3), the point (x, y) on the boundary line of ellipse element is expressed as follows :

$$x=a\cos\left[\tan^{-1}\left(\frac{a}{b}\tan\beta\right)\right] \cdots\cdots (A\text{-}5a)$$

$$y=b\sin\left[\tan^{-1}\left(\frac{a}{b}\tan\beta\right)\right] \cdots\cdots (A\text{-}5b)$$

When the local coordinate in which the x-axis coincides with the apsides of ellipse element rotates as shown in **Fig.A-2**, the angle β becomes

$\beta=\theta-\phi$.

Therefore,

$$x=a\cos\left[\tan^{-1}\left\{\frac{a}{b}\tan(\theta-\phi)\right\}\right] \cdots\cdots (A\text{-}6a)$$

$$y=b\sin\left[\tan^{-1}\left\{\frac{a}{b}\tan(\theta-\phi)\right\}\right] \cdots\cdots (A\text{-}6b)$$

REFERENCES

1) Sabo and Landslide Technical Center:Steel-made Sabo Structure Design Manual, Oct.1985 (in Japanese).
2) Kiyama, H. and Fujimura, H. : The Analysis of the Gravity Flow of Granular Rock Assemblies using Cundall's Model, Proc. of JSCE, No.333, pp.137-146, May 1983 (in Japanese).
3) Cundall, P.A.:A Computer Model for Simulating Progressive Large Scale Movements in Blockey Rock Systems, Symp. ISRM, Nancy, France, Proc., Vol.2, pp.129-136, 1971.
4) Meguro, K. and Hakuno, M.:Fracture Analysis of Concrete Structures by the Modified Distinct Element Method, Structural Eng./Earthquake Eng., Vol.6, No.2, pp.283-294, Oct.1989, JSCE. (Proc. of JSCE No.410/I-12).
5) Omachi, T. and Arai, Y.:On the Determination of Element Coefficient in the Distinct Element Model, Proc. of Structural Engineering, Vol.32A, pp.715-723, March 1986 (in Japanese).
6) Yoshida, H., Masuya, H. and Imai, K.:Impulsive Properties of Falling Rocks on Sand-Layers by Means of Cundall's Discrete Block Method, Proc. of JSCE, No.392/I-9, pp.297-306, April 1988 (in Japanese).
7) Togawa, H.:Vibrational Analysis by Finite Element Analysis, Science Co. Ltd., 1975 (in Japanese).

(Received September 27, 1990)